SOLITARY WAVES AND BORES PASSING THREE CYLINDERS - EFFECT OF DISTANCE AND ARRANGEMENT

Stefan Leschka[1] and Hocine Oumeraci[2]

Depth-averaged models such as non-linear shallow water (NLSW) and Boussinesq based codes usually use the quadratic friction law with Manning's coefficient to describe the surface roughness of the bottom. Large roughness elements such as buildings and tree vegetation, which are too small to be resolved by the grid of the bottom topography, are mainly considered by using purely empirical Manning coefficients. This approach, however, is not physically sound and may thus result in very large uncertainties in inundation modeling. A more physically-based approach is to determine prediction formulae for the hydraulic resistance of large roughness elements, considering for example different shapes, sizes and arrangements which can then be directly implemented in such models. Such prediction formulae can be determined on the basis of systematic simulations using a validated 3D numerical model. To better understand complex flow phenomena involved in tsunami inundation, three vertical emerged cylinders have been arranged in four different configurations with four different distances between each other and subject to a solitary wave and to a bore. A validated three-dimensional two-phase Reynolds-averaged Navier-Stokes (RANS) model and the Volume of Fluid (VOF) method (OpenFOAM) has been used to assess flow velocities and water levels near the cylinders and the inline forces acting on the cylinders. The effects of side-by-side, tandem and two staggered arrangements as well as the effect of the distances between them on the flow induced by a solitary wave and a bore are discussed. The study led to an improved understanding in the near field of cylinders, which forms the basis for further studies related to larger groups of cylinders and other shapes.

Keywords: vertical emerged cylinders; solitary waves; bores; RANS models

INTRODUCTION

Propagating tsunamis are influenced by wave characteristics such as wave period and wave direction, the seabed topography and morphologies, such as shoals and reefs, underwater canyons and man-made structures can cause large changes in wave height and direction of travel. The interaction of the seabed with the wave can cause wave attenuation and breaking.

Flooding waves on land, such as tsunamis or storm surges, interact with a complex onshore morphology, for example dunes, coastal forests, man-made structures such as seawalls, dikes or buildings. The correct implementation of these interactions is essential for predicting tsunami height and inundation, because they affect results up to the first order, e.g. Satake et al. (1993), Yeh et al. (1993) and Synolakis et al. (1995).

For example in tsunami risk assessment, large-scale tsunami models are mainly depth-averaged models such as Non-linear shallow water (NLSW) models or Boussinesq models can be applied. Due to their size, their resolution is often limited so that the grid of the bottom topography cannot represent adequately smaller morphologies such as buildings and tree vegetation. These so-called large roughness elements need, in turn, to be considered with the help of empirical relations, which are added to the governing equations. To date, models use mainly the concept of the boundary surface roughness. They apply for example modified Manning coefficients to account for the interactions of the broken or unbroken wave with the bottom and smaller morphologies (e.g. Chow (1959), Harada & Imamura (2000), Latief (2000), Choi et al. (2009), Gayer et al. (2010), Jakeman et al. (2010) and Kaiser et al. (2011)). In this concept, losses are related to the water depth, which is only represented in the grid nodes, assuming that the water depth between the nodes is similar. However, with the presence of large roughness elements this assumption no longer holds. This makes predictive modelling of tsunami inundation und risk assessment with the help of large scale models very difficult.

Large roughness elements in relation to the water depth have been investigated e.g. by Matsutomi et al. (2006), Augustin et al. (2009), Yuan & Huang (2009), Suzuki & Arikawa (2010) and Husrin et al. (2012). A framework has been outlined in which empirical relations for a more physically sound representation of large roughness elements will be developed (Leschka & Oumeraci 2011). As part of this framework, basic parameter tests involving three cylinders subject to a solitary wave and a bore have been performed to better understand the interaction between roughness elements. A well-validated 3-dimensional (3D) Reynolds-averaged Navier-Stokes (RANS) model has been used for this purpose.

[1] Hydrodynamics & Coastal engineering, DHI-WASY GmbH, Max-Planck-Str. 6, 28857 Syke, Germany
[2] Leichtweiss-Institute for Hydraulic Engineering & Water Ressources, TU Braunschweig, Beethovenstr. 51a, 38106 Braunschweig, Germany

The sections of the here presented study describe the numerical setups and the results, which will finally be discussed.

NUMERICAL MODEL

The open source CFD software package OpenFOAM has been used as a numerical framework in this study. From this package, the solver interFoam for multiphase incompressible, isothermal and immiscible flow is based on the 3D RANS equations has been used. The water surface is captured with the volume of fluid (VOF) method (Olsson & Kreiss 2005; Olsson et al. 2007). Turbulence has been estimated with the k- ω-SST model.

The model has been validated with an extensive program. Laboratory data from Large Wave Flume (GWK) of the coastal Research Centre (FZK) in Hanover, the wave flume of Leichweiss Institute for Hydraulic Engineering & Water Ressources (LWI) at TU Braunschweig involving single cylinders subject to regular waves and two to three cylinders in various arrangements (Bonakdar, 2012; Bonakdar & Oumeraci, 2014) have been used. Laboratory tests of a solitary wave passing a submerged reef structure (Strusinska, 2010) have been used to validate wave generation and to minimize numerical dissipation. Laboratory data of a bore acting on a single cylinder, performed at Charles W. Harris Laboratory of the University of Washington have been made available (Yeh, 2014). A detailed description of the validation is given in Leschka et al. (2014).

Numerical setups

Three emerged cylinders with a diameter of D_B = 0.05m. They are arranged in side-by-side, tandem and two staggered configurations, shown in figure 1.

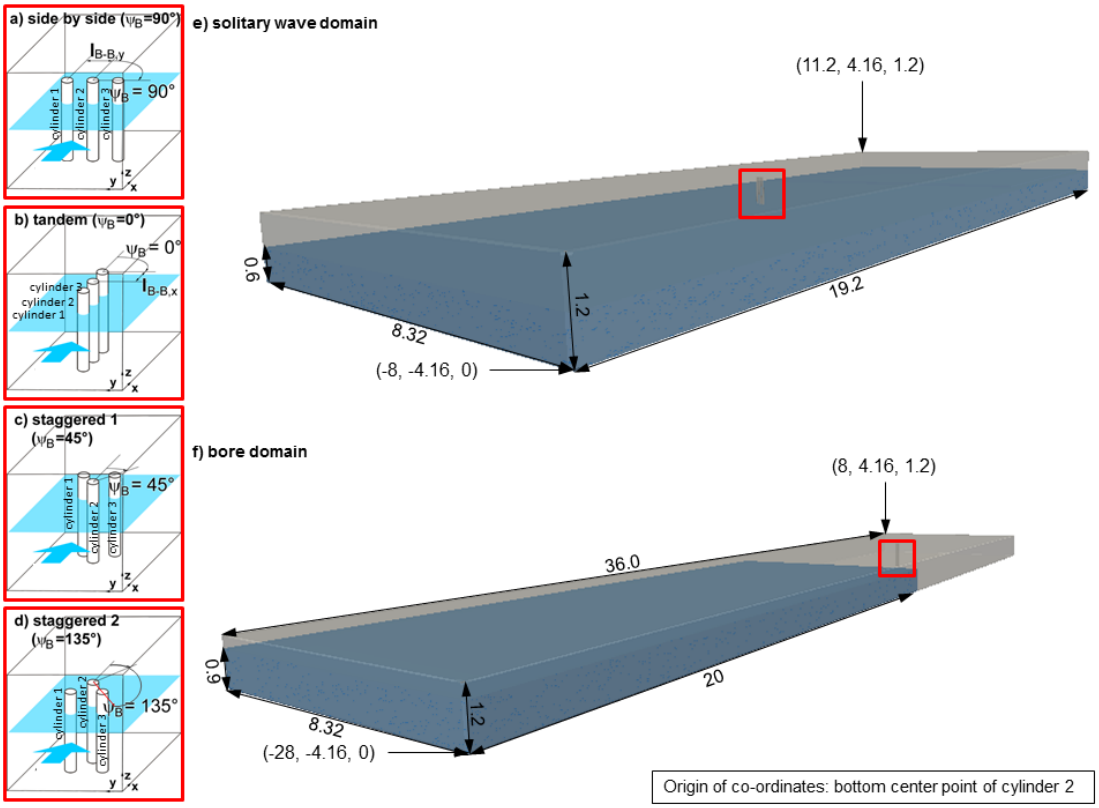

Figure 1. Basic types of arrangements of cylinders.

The arrangement is expressed using the arrangement angle Ψ_B, which has its origin at the middle roughness element at (x, y) = (0, 0) and spans clockwise between the direction in which the flow goes to and the direction in which the next roughness element is encountered. The distance between the elements $l_{B\text{-}B}$ takes the values of 0.5 D_B, 1 D_B, 2 and 3 D_B. For comparison, 2 additional simulations

have been further considered which comprise of a single cylinder at (x, y) = (0, 0). This results in a total of 34 simulations.

The numerical domain characteristics of the solitary wave and bore cases are summarized in table 1 and presented in figure 1.e) and f), respectively.

Table 1. Characteristics of numerical domains.

	Solitary wave	Bore
X	{-8, …, 11} m	{-28, …, 8} m
Y	{-4.16, …, 4.16} m	{-4.16, …, 4.16} m
Z	{0, … 1.2} m	{0, …, 1.2} m

The solitary wave has been 0.22 m high and the still water depth has been 0.6 m (see figure 1.e)). It has been generated using the solver waveFoam (Jacobsen et al 2012). The bore was generated with a dambreak mechanism, setting an initial water block of 20 m length and 0.9 m height in a distance of 8 m from the middle cylinder (see figure 1.f)).

The forces have been calculated in all three cylinders using the function object of type "forces". The results are presented in the following section.

RESULTS

The maximum inline forces in all cases of three cylinders subject to solitary waves and bores have been normalized with the maximum force of the corresponding single cylinder case using the relation

$$F^*(x)_{cylinderi,\max} = \frac{F(x)_{cylinderi,\max}}{F(x)_{1cylinder,\max}} \qquad (1)$$

In Eq. (1), $F(x)_{\text{cylinder i,max}}$ is the maximum inline force cylinder i and $F(x)_{1\text{ cylinder,max}}$ is the maximum inline force in the single cylinder case.

In the solitary wave cases, the maximum force is reached when the wave crest passes the cylinders and maximum flow velocities can be observed in the vicinity. In case of bores, the maximum inline force has also been observed at high water levels. In the moment of impact the flow velocities are very high, but the water level has been low which resulted in a peak smaller than then the one observed at higher water levels when the bore passed by. The results have been analyzed related to the relative distance of the cylinders $x_{B\text{-}B}/D_B$ and to the arrangement angle Ψ_B.

Influence of the distance on maximum inline forces

Tandem Arrangement

Figure 2 presents the normalized maximum inline forces in three cylinders in tandem arrangement under the conditions of a solitary wave and a bore.

The middle cylinder (cylinder 2, see figure 1.b)) receives the smallest force in both flow regimes, whereas the first cylinder (cylinder 1) receives the highest. The distance between the cylinders plays a minor role for bores. In case of a solitary wave, the differences between the cylinders vanish when the spacing becomes 3 D_B. In the bore case the difference between the first and the following cylinders is apparent for all investigated distances. At these distance, cylinders 2 and 3 benefit from standing in tandem arrangement. The differences between solitary wave and bore cases might arise from different flow velocities. They have been analyzed in representative horizontal planes around the cylinders. In case of solitary waves, the velocities have been analyzed at half still water depth (z = 0.3 m), in case of bores at z = 0.05 m. Figure 3 and figure 4 present flow fields around the cylinders in tandem arrangement subject to the solitary wave and the bore, respectively.

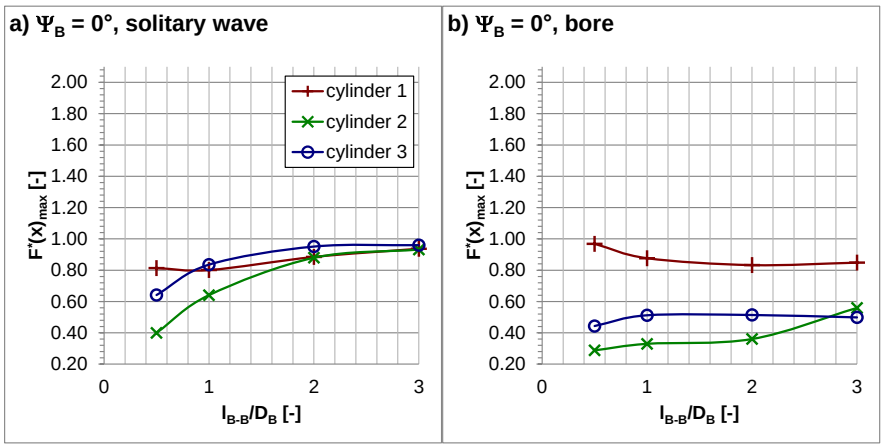

Figure 2. Normalized max. inline forces correlated with the relative cylinder distance for tandem arrangement: a) solitary wave; b) bore (modified from Leschka et al., 2014, copyright @ 2014 World Scientific).

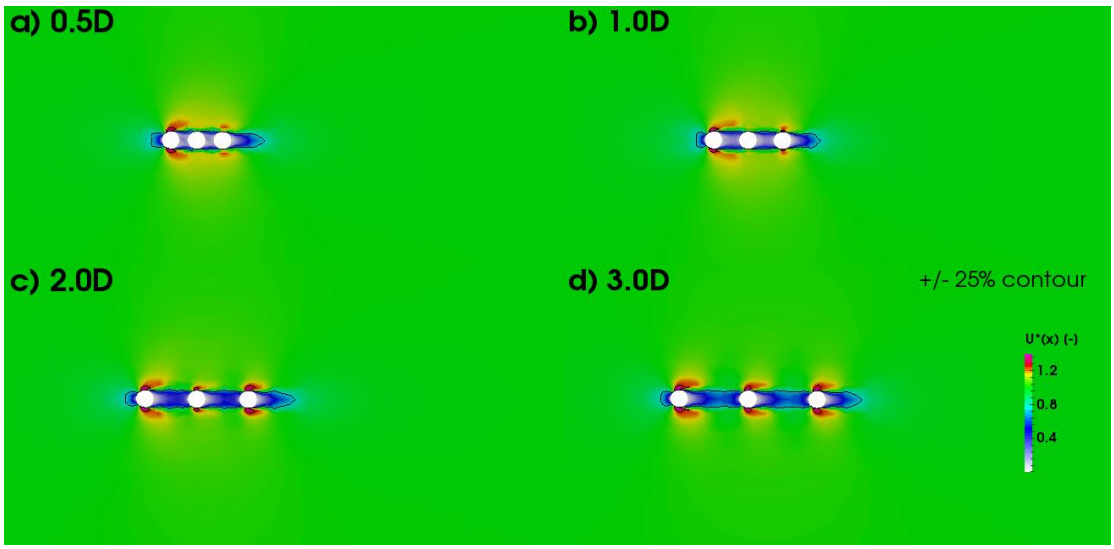

Figure 3. Normalized maximum flow velocities around cylinders in tandem arrangement subject to a solitary wave. The black line indicates the boundary at which maximum flow velocities are by 25 % higher or lower compared to the case without cylinders (Leschka et al., 2014, copyright @ 2014 World Scientific).

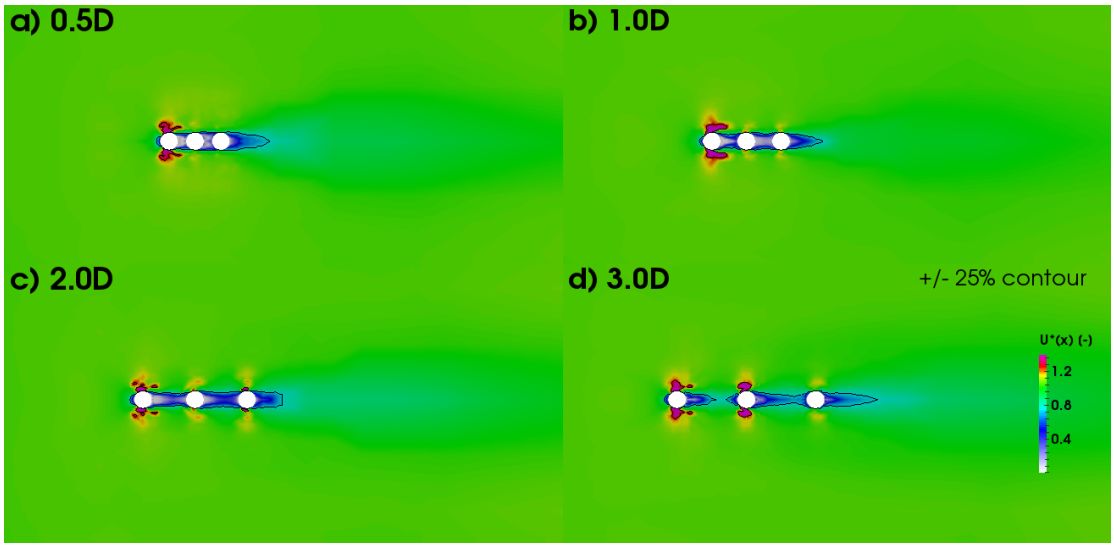

Figure 4. Normalized maximum flow velocities around cylinders in tandem arrangement subject to a bore. The black line indicates the boundary at which maximum flow velocities are by 25 % higher or lower compared to the case without cylinders (Leschka et al., 2014, copyright @ 2014 World Scientific).

In case of bores the zones in which the flow velocities are reduces extend further downstream. The velocities in the bore have been higher and thus the inertia of the water particles is greater than in the solitary wave regime. Once the particles have been deflected by the first cylinder, they tend to move in the mean flow direction and travel a longer distance before moving back into the sheltered area downstream of the cylinder. That's why in a bore the second and third cylinder benefit from the shelter of the first cylinder over greater distances than in the solitary wave cases.

Staggered 1 arrangement

Figure 5 presents the normalized maximum inline forces in three cylinders in staggered 1 arrangement under the conditions of a solitary wave and a bore.

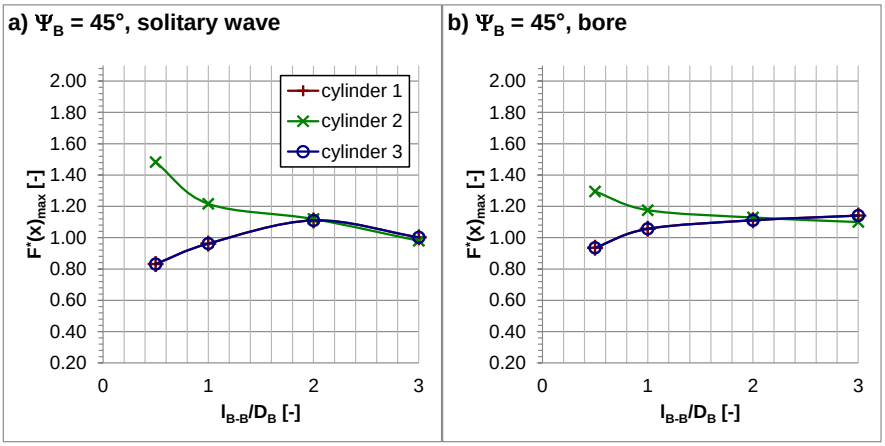

Figure 5. Normalized max. inline forces correlated with the relative cylinder distance for staggered 1 arrangement: a) solitary wave; b) bore (modified from Leschka et al. 2014, copyright @ 2014 World Scientific).

The middle cylinder, placed at the furthest upstream position (see figure 1.c)), receives the highest force in both flow regimes. The differences between the cylinders vanish when the distance becomes 2 D_B. Similar to the tandem arrangement, the flow velocities have been analyzed around the cylinders. They are represented in figure 6 for the solitary wave cases and in figure 7 for the bore cases.

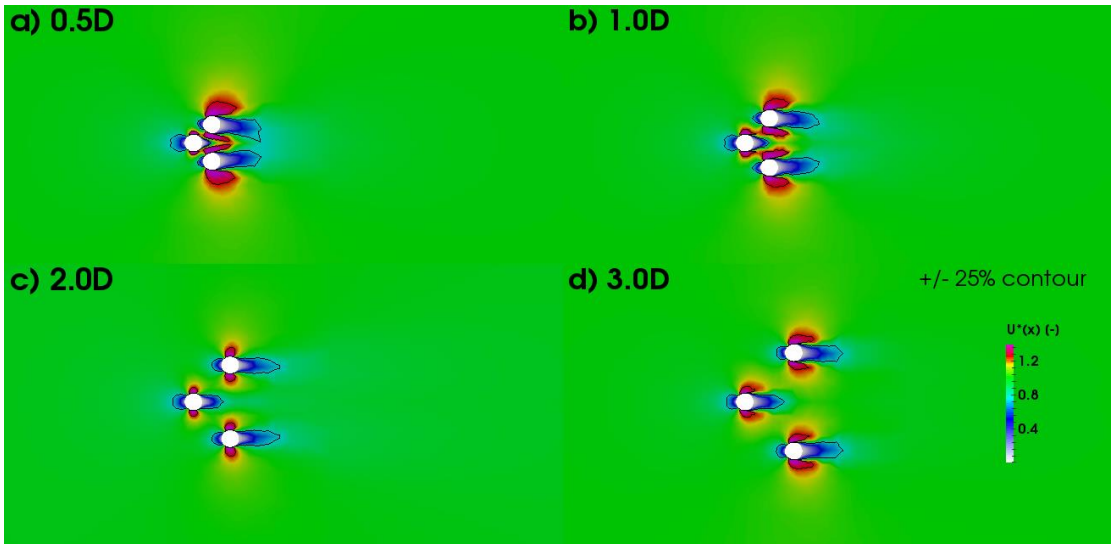

Figure 6. Normalized maximum flow velocities around cylinders in staggered1 arrangement subject to a solitary wave. The black line indicates the boundary at which maximum flow velocities are by 25 % higher or lower compared to the case without cylinders (Leschka et al., 2014, copyright @ 2014 World Scientific).

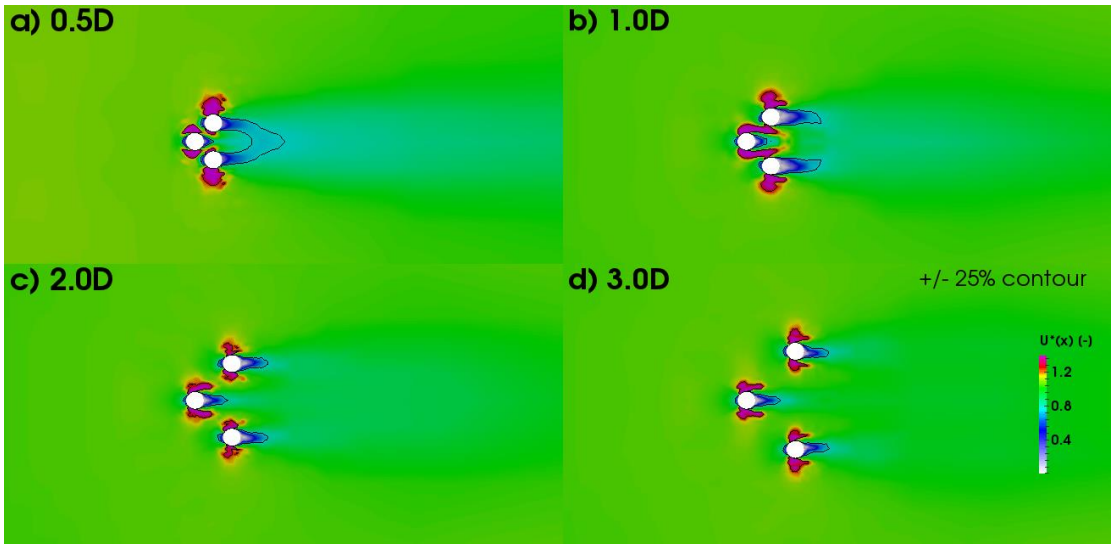

Figure 7. Normalized maximum flow velocities around cylinders in staggered1 arrangement subject to a bore. The black line indicates the boundary at which maximum flow velocities are by 25 % higher or lower compared to the case without cylinders (Leschka et al., 2014, copyright @ 2014 World Scientific).

A physical interpretation is that the interference between the cylinders is important as long the outer cylinders lie in the wake of the middle cylinder. When water particles near the outer cylinders are forced to move around them, a force results which is deflected relative to the free stream direction. Hence, there is a component of the force acting orthogonally to the free stream direction, called a lift force (Zdravkovich 1977). Hori (1959) investigated the pattern of drag and lift coefficients for various staggered arrangements with cylinders subject to wind. He drew the interference force coefficients for all of his arrangements and indicated direction and magnitude of the coefficients, which is recalled in figure 8.

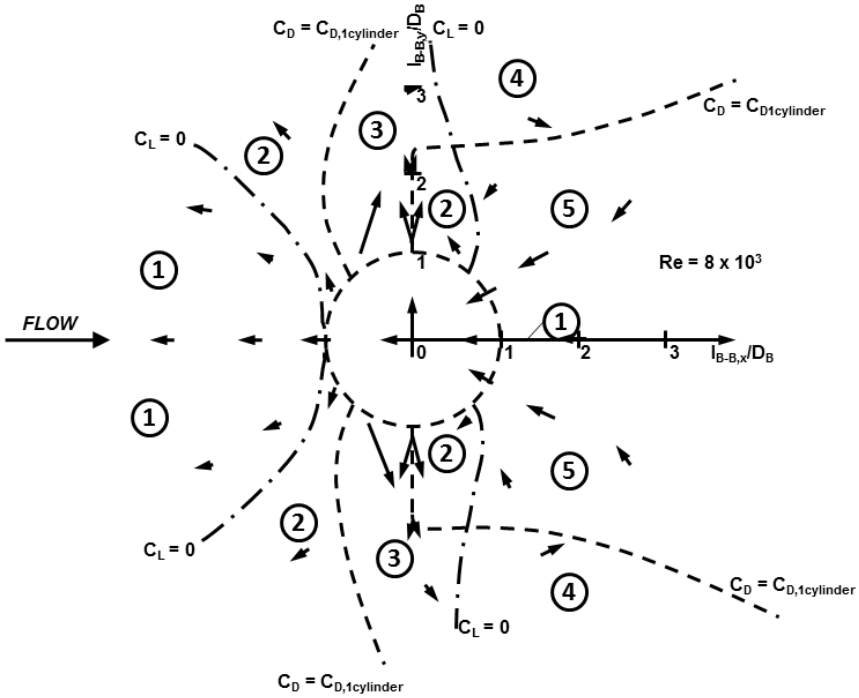

Figure 8. Interference force coefficient for all arrangements (modified from Hori (1959)).

In this figure, five zones can are identified: (1) Negligible lift force and reduced drag force, (2) Small repulsive lift force and reduced drag force, (3) Repulsive lift force and increased drag force, (4) Negligible lift force and increased drag force and (5) Negative lift force and decreased drag force.

When cylinder 2 is placed at the origin of the coordinate system, it receives interference forces from cylinders 1 and 3, which are located in zone 5. This further explains the reduced forces in the outer cylinders for $l_{B\text{-}B}/D_B < 2$.

Side-by-side arrangement

Figure 9 presents the normalized maximum inline forces in three cylinders in side-by-side arrangement under the conditions of a solitary wave and a bore.

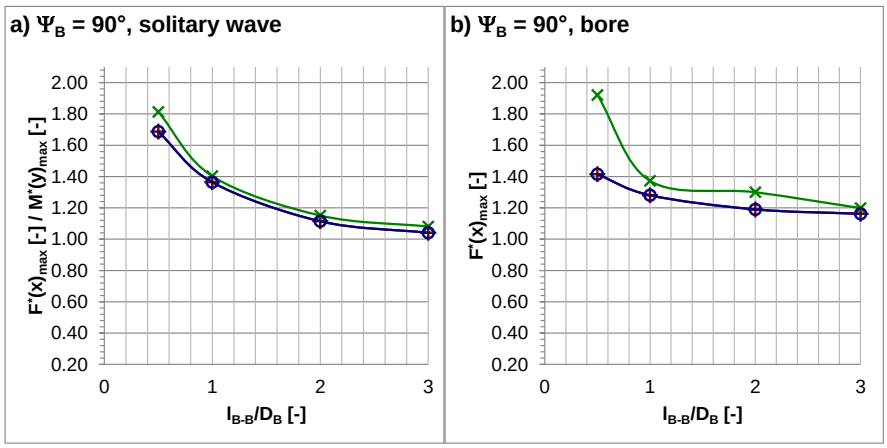

Figure 9. Normalized max. inline forces correlated with the relative cylinder distance for side-by-side arrangement: a) solitary wave; b) bore (modified from Leschka et al. 2014, copyright @ 2014 World Scientific).

The middle cylinder (see figure 1.a)) receives the highest load. The forces acting on the cylinders decrease with increasing distance. While the differences in case of a solitary wave are small, they are more apparent in the bore cases. While the force in cylinders subject to a solitary waves approach a value close to the one of a single cylinder, in case of bores forces are higher in all cylinders than in a single cylinder. For further insights in these phenomena, the flow fields are given in figures 10 and 11.

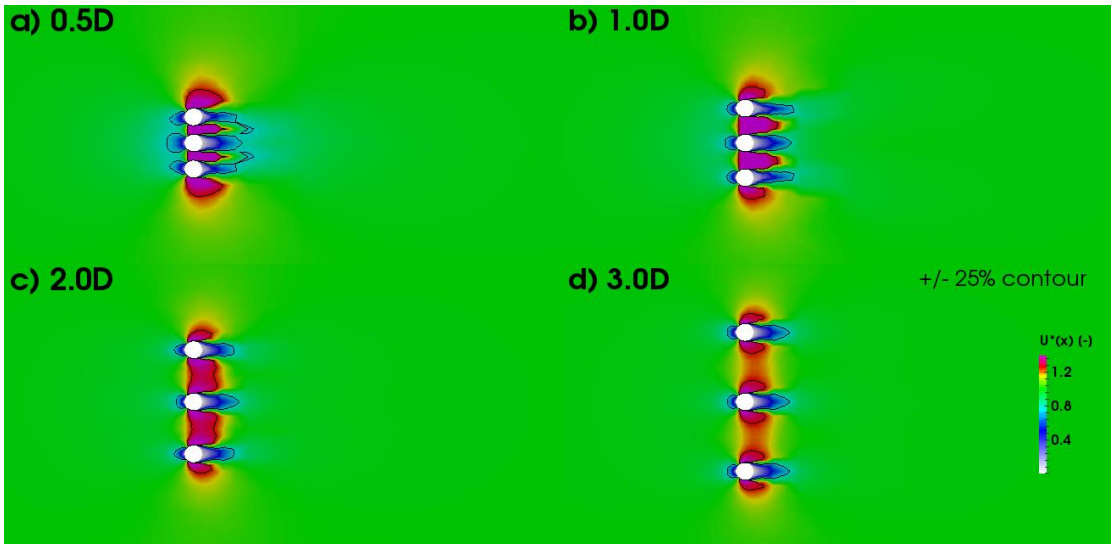

Figure 10. Normalized maximum flow velocities around cylinders in side-by-side arrangement subject to a solitary wave. The black line indicates the boundary at which maximum flow velocities are by 25 % higher or lower compared to the case without cylinders (Leschka et al., 2014, copyright @ 2014 World Scientific).

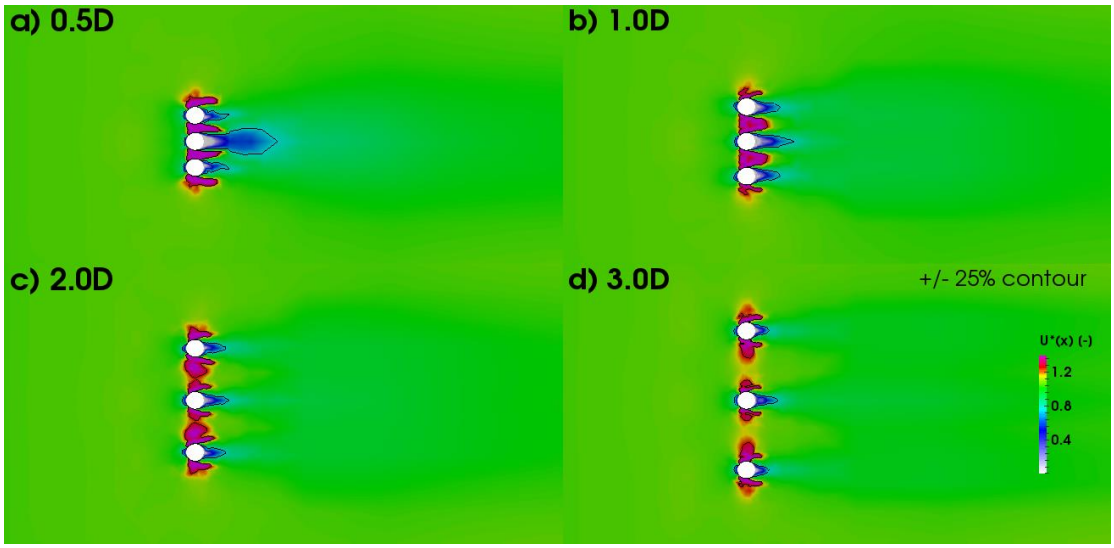

Figure 11. Normalized maximum flow velocities around cylinders in side-by-side arrangement subject to a bore. The black line indicates the boundary at which maximum flow velocities are by 25 % higher or lower compared to the case without cylinders (Leschka et al., 2014, copyright @ 2014 World Scientific).

Especially when looking at the wakes behind each cylinder it can be seen, that the length behind the outer cylinders is smaller than behind the middle cylinder. These differences are more apparent in the bore cases.

The interference between the cylinders prevents the water particles to move around the cylinders, as they would do around a single isolated cylinder. The water particles have to move through the space between two cylinders at the same time. This leads to higher water levels at the upstream cylinder face

and higher velocities in the space between than in case of single cylinders. Zdravkovich (1977) reported a similar behavior and found that the trend is independent from Re and that the cylinders influence each other even at a spacing of $l_{B\text{-}B}/D_B = 5$.

Staggered 2 arrangement

Figure 12 presents the normalized maximum inline forces in three cylinders in staggered 2 arrangement under the conditions of a solitary wave and a bore.

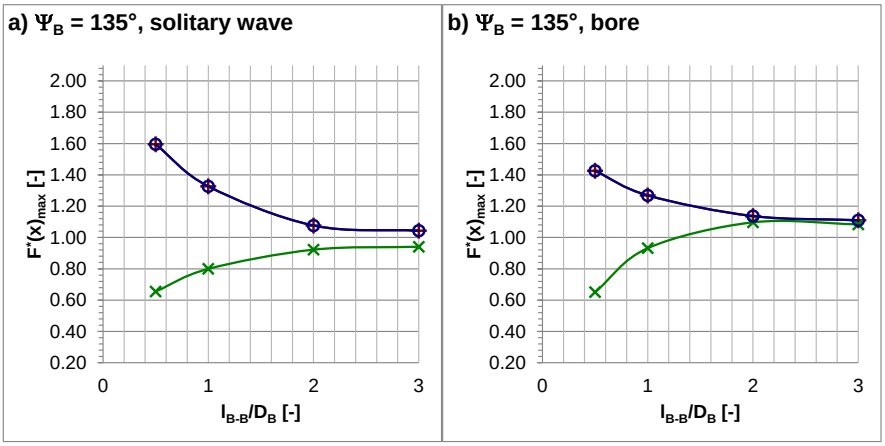

Figure 12. Normalized max. inline forces correlated with the relative cylinder distance for staggered 2 arrangement: a) solitary wave; b) bore (modified from Leschka et al. 2014, copyright @ 2014 World Scientific).

The deviation between the inline forces in the cylinders is larger the closer the cylinders stand together. At a distance of $l_{B\text{-}B}/D_B = 0.5$, the largest force can be observed in the outer cylinders; the smallest force can be observed in the middle cylinder (cylinder 2, placed in the background). From 2 D_B onwards the differences between the cylinders are very small. In the solitary wave case they take values close to the forces of the single cylinder. The force in the bore cases show similar behavior, but at a distance of 3 D_B they are slightly higher than found in a single cylinder. The flow fields around the cylinders prove this behavior. They are given in figure 13 for a solitary wave and in figure 14 for a bore.

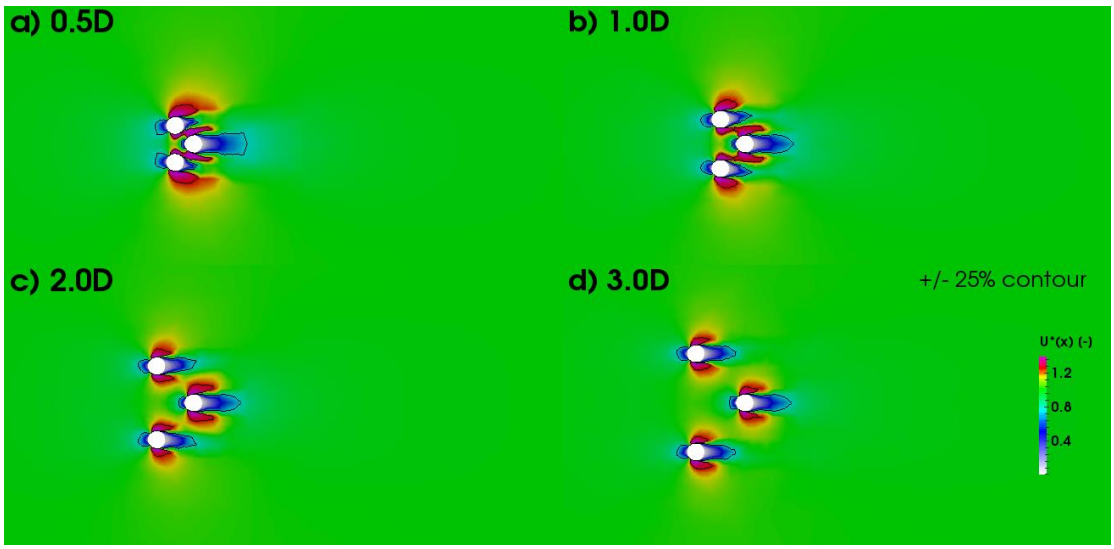

Figure 13. Normalized maximum flow velocities around cylinders in staggered 2 arrangement subject to a solitary wave. The black line indicates the boundary at which maximum flow velocities are by 25 % higher or lower compared to the case without cylinders (Leschka et al., 2014, copyright @ 2014 World Scientific).

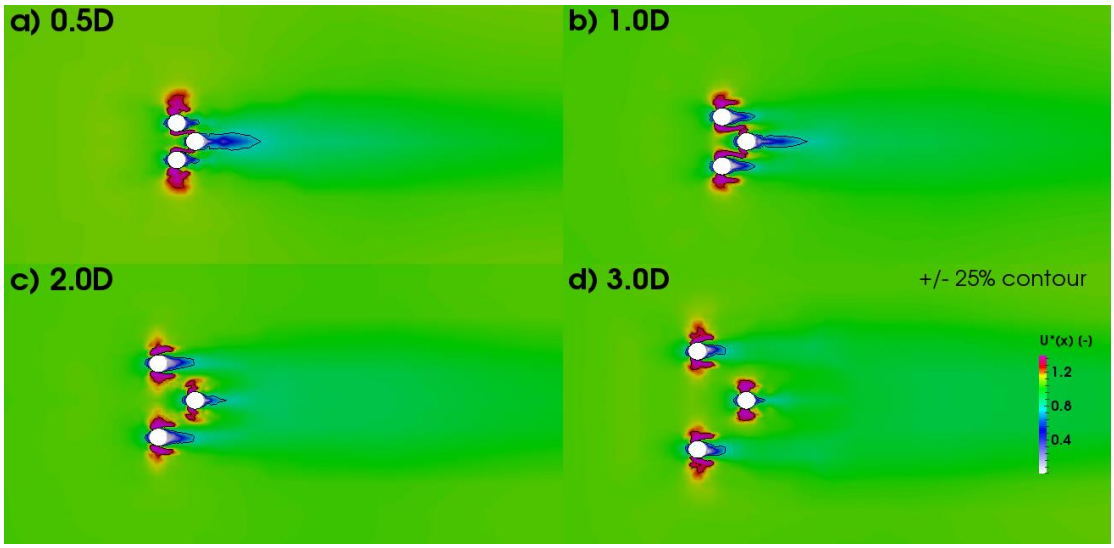

Figure 14. Normalized maximum flow velocities around cylinders in staggered 2 arrangement subject to a bore. The black line indicates the boundary at which maximum flow velocities are by 25 % higher or lower compared to the case without cylinders (Leschka et al., 2014, copyright @ 2014 World Scientific).

The flow fields around each cylinder become more similar with increasing cylinder spacing.

Because the flow is forced to move around the outer cylinder, an additional force acts on the outer cylinders. The interference force pattern in figure 8 confirms that the outer cylinders receive higher loads than the middle cylinder.

The slopes of the curves in figure 2 indicate that the influence of the distance between the cylinders is more apparent under solitary wave conditions, except when they stand side-by-side. Here, the forces in the middle cylinder are increased to a larger extend under bore conditions.

Influence of the type of arrangement on maximum inline forces

The normalized maximum inline forces of the tests in all arrangement types with both flow patterns are given in figure 15.

For both flow regimes it can be noted that the deviation from forces in a single cylinder case decrease with decreasing distance. The influence of the arrangement angle on the forces is also more pronounced in cases of smaller distances. When analyzing the slope of the trend lines it is noted that the effect of the arrangement type is larger in bore cases than for solitary waves. The forces in all cylinders increase under both flow regimes, the closer the arrangement angle reaches 90° (side-by-side).

It can further be noted that the normalized forces in all cylinders in tandem and side-by-side arrangements differ less among each other than in the staggered arrangements. They decrease with increasing distance.

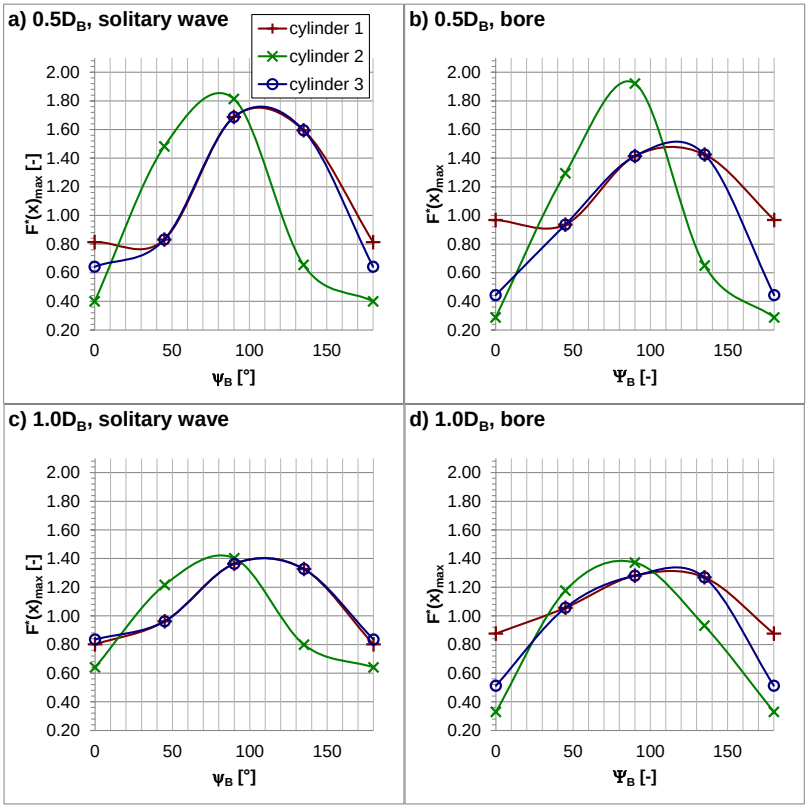

Figure 15. Normalized max. inline forces correlated with the arrangement: a) 0.5DB, solitary wave; b) 0.5DB, bore; c) 1.0DB, solitary wave; d) 1.0DB, bore; e) 2.0DB, solitary wave; f) 2.0DB, bore; g) 3.0DB, solitary wave; h) 3.0DB, bore (modified from Leschka et al. 2014, copyright @ 2014 World Scientific).

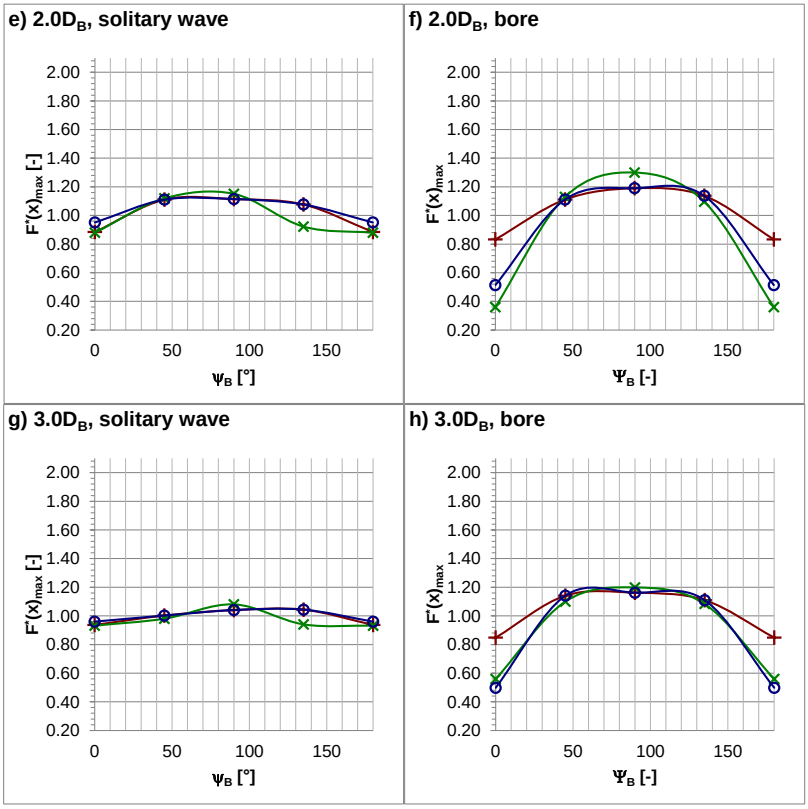

Figure 15. continued.

SUMMARY AND CONCLUSION

The forces on three cylinders subject to a solitary wave and a bore have been investigated as a function of the type of group arrangement and the distance between the cylinders in this study. A 3D RANS model, validated in Leschka et al. (2014), has been applied.

When the normalized maximum forces are related to the distance between the cylinders, differences among them are more pronounced under solitary wave conditions, except in the side-by-side arrangement with a distance of 0.5 D_B. Forces on the cylinder tend to increase when the arrangement angle is around 90° (side-by-side arrangement). When the normalized maximum forces are related to the arrangement, the opposite behavior can be noted. The differences among the arrangements differs more in case of bores.

In order to quantify the influence of the parameters distance and arrangement on the inline forces for each flow regime, the standard deviation s has been determined for all forces. The higher the standard deviation of values obtained from a group of quantities is, the larger is the difference between the forces. It can be used to indicate the influence of a certain parameter. The standard deviations over the investigated arrangement angles (in rows) and over the distances (in columns) are presented in table 2 for cylinder 1, in table 3 for cylinder 2 and in table 4 for cylinder 3.

Table 2. Standard deviations of forces in cylinder 1 for different distances between cylinders and types of arrangements (Leschka et al., 2014).

Solitary wave						Bore				
σ	0	45	90	135	D_B	0	45	90	135	σ
0.41	0.81	0.83	1.69	1.59	0.5	0.97	0.94	1.41	1.43	0.23
0.24	0.80	0.96	1.36	1.33	1	0.88	1.06	1.28	1.27	0.17
0.09	0.88	1.11	1.11	1.08	2	0.83	1.11	1.19	1.14	0.14
0.04	0.94	1.00	1.04	1.04	3	0.85	1.14	1.16	1.11	0.13
	0.06	0.10	0.25	0.22	σ	0.05	0.08	0.10	0.13	

Table 3. Standard deviations of forces in cylinder 2 for different distances between cylinders and types of arrangements (Leschka et al., 2014).

Solitary wave						Bore				
σ	0	45	90	135	D_B	0	45	90	135	σ
0.58	0.40	1.48	1.81	0.65	0.5	0.29	1.29	1.92	0.65	0.62
0.31	0.64	1.22	1.40	0.80	1	0.33	1.18	1.37	0.93	0.39
0.12	0.88	1.12	1.15	0.92	2	0.36	1.13	1.30	1.10	0.36
0.06	0.93	0.98	1.08	0.94	3	0.56	1.10	1.20	1.08	0.25
	0.21	0.18	0.29	0.11	σ	0.10	0.07	0.28	0.18	

Table 4. Standard deviations of forces in cylinder 3 for different distances between cylinders and types of arrangements (Leschka et al., 2014).

Solitary wave						Bore				
σ	0	45	90	135	D_B	0	45	90	135	σ
0.46	0.64	0.83	1.69	1.59	0.5	0.44	0.94	1.41	1.43	0.41
0.23	0.84	0.96	1.36	1.33	1	0.51	1.06	1.28	1.27	0.31
0.07	0.95	1.11	1.11	1.08	2	0.51	1.11	1.19	1.14	0.28
0.03	0.96	1.00	1.04	1.04	3	0.50	1.14	1.16	1.11	0.28
	0.13	0.10	0.25	0.22	σ	0.03	0.08	0.10	0.13	

When comparing standard deviations considering all investigations of the arrangement by averaging, it leads to the summary presented in table 5.

For the solitary wave, type of arrangement and distance between cylinders have comparable effects on the forces whereas in case of bores the effect of the arrangement type dominates. Generally, the effect of the arrangement type on the loading of the cylinders is higher than that of the distance between cylinders.

Table 5. Standard deviations of forces in cylinder 3 for different distances between cylinders and types of arrangements (Leschka et al., 2014).

	Solitary wave	Bore
Ψ_B	0.22	0.30
$l_{B\text{-}B}/D_B$	0.18	{0.11

ACKNOWLEDGEMENTS

The first author like to thank DHI Water & Environment Singapore for providing resources and time to work on this topic, Agnieszka Strusinska-Correia, Prof. Harry Yeh and Lisham Bonakdar for providing experimental data and for fruitful discussions. Furthermore, he likes to thank Hisham El-Safti and Prof. Ioan Nistor for open discussions. The funding of the German Research Foundation (DFG, Deutsche Forschungsgemeinschaft) for the WaPiGS project and HYBTEW project is gratefully acknowledged by the second author.

REFERENCES

Árnason, H., 2004. Interactions between an Incident Bore and a Free-Standing Coastal Structure, Ph.D. thesis, University of Washington, USA.

Árnason, H., Yeh, H. and Petroff, C. 2005. Interactions between an Incident Bore and a Vertical Column, http://people.oregonstate.edu/~yehh/tsunamiforces/, last accessed: June 13, 2014.

Augustin, L.N., Irish, J.L. and Lynett P.J. 2009. Laboratory and numerical studies of wave damping by emergent and near-emergent wetland vegetation, *Coastal Engineering*, 56, 332-340.

Bonakdar, L. 2012, personal communication, 19/10/2013 18:32 CET.

Bonakdar, L. and Oumeraci, H. 2014. Small and large scale experimental investigations of wave loads on a slender pile withinclosely spaced neighbouring piles, *Proceedings of 33rd International Conference on Ocean, Offshore and Arctic Engineering*, San Francisco, California.

CFD-Wiki. 2012. Turbulence free stream boundary conditions, http://www.cfd-online.com/Wiki/Turbulence_free-stream_boundary_conditions, last accessed: 27 February 2014.

Choi, J. and Yoon, S.B. 2009. Numerical simulations using momentum source wave-maker applied RANS equation model, *Coastal Engineering*, 56, 1043-1060.

Chow, V. 1959. *Open Channel Hydraulics*, McGraw Hill, New York.

Dean, R.G. and Dalrymple, R.A. 1991. *Water Wave Mechanics for Engineers and Scientists, Advanced Series on Ocean Engineering*, World Scientific, Singapore.

Gayer, G., Leschka, S., Noehren, I., Larsen, O. and Guenther, H. 2010. Tsunami inundation modelling based on detailed roughness maps of densely populated areas, *Natural Hazards & Earth System Science*, 10, 1679-1687.

Harada, K. and Imamura, F. 2000. Experimental study on the resistance by mangrove under the unsteady flow, *Proceedings of the 1st Congress of APACE*, pp. 975-984.

Hori, E. 1959. Experiments on Flow around Pair of Parallel Circular Cylinders, *Proceedings of 9th Japan National Congress for Applied Mechanics*, Tokyo, pp. 231-234.

Husrin, S., Strusinska, A. and Oumeraci, H. 2012. Experimental study on tsunami attenuation by mangrove forest. *Earth Planets Space*, 64, 973-989.

Jacobsen, N.G., Furmann, D.R. and Fredsoe, J. 2012. A wave generation toolbox for the Open-Source CFD Library: OpenFOAM. *Int. J. Numerl. Meth. Fluids*, 70(9), 1073-1088.

Jakeman. 2010, J.D., Nielsen, O.M., can Putten, K., Mleczko, R., Burbidge, D. and Horspool, N. 2010. Towards spatially distributed quantitative assessment for tsunami inundation models. *Ocean Dyn.*, 60, 1115-1138.

Kaiser, G., Scheele, L., Kortenhaus, A., Løvolt, F., Roemer, H. and Leschka, S. 2011. The influence of land cover roughness on the resultof high resolution tsunami inundation modeling. *Nat. Hazards Earth Syst. Sci.*, 11, 2521–2540.

Latief, H. 2000. Study on tsunamis and their mitigation by using a green belt in Indonesia. Ph.D. thesis, Tohoku University, Sendai, Japan

Leschka, S. and Oumeraci, H. [2011] "3D numerical simulations of the effect of large roughness elements on the propagation of solitary waves,"6th Annual Int. Workshop and Expo on Sumatra Tsunami Disaster and Recovery 2011 in Conjunction with 4th South China Sea Tsunami

Workshop, Banda Aceh, Indonesia, available at http://www.dhi-ntu.com.sg/-/media/publications/news/2013/04/leschkaoumeraci_2011-effectoflargerougnesselementsonthepropagationofsolitarywaves.pdf (accessed on September 24, 2014)

Leschka, S., Oumeraci, H. and Larsen, O. 2014. Hydrodynamic Forces on a Group of Three Emerged Cylinders by Solitary Waves and Bores: Effect of Cylinder Arrangements and Distances. *Journal of Earthquake and Tsunami*, 8 (3), 144005 (36 pages).

Matsutomi, H., Ohnuma, K., Suzuki, A. and Imai, K. 2006. Governing equations for inundated flow in vegetated areas and similarity laws for tree trunks. *Proceedings of 30th Int. Conf. Coastal Engineering*, San Diego, California.

Olsson, E. and Kreiss, G. 2005. A conservative level set method for two phase flow. *J. Comput. Phys.*, 210, 225–246.

Olsson, E., Kreiss, G. and Zahedi, S. 2007. A conservative level set method for two phase flow II. *J. Comput. Phys.*, 225, 785-807.

Satake, K., Bourgeois, J., Abe, Ku., Abe, Ka., Tsuji, Y., Imamura, F., Iito, Y., Katao, H., Noguera, E. and Estrada, F. 1993. Tsunami field survey of the 1992 Nicaragua Earthquake. *EOS Trans. Am. Geophys. Union*, 74 (13), 145–160.

Strusinska, A. 2010. Hydraulic Performance of an Impermeable Submerged Structure for Tsunami Damping. Ph.D. thesis, TU Braunschweig, Germany.

Suzuki, T. and Arikawa, T. 2010. Numerical analysis of bulk drag coefficients in dense vegetation by immerse boundary method. *Proceedings of 32 Int. Conf. Coastal Engineering*, Shanghai, China.

Synolakis, C. E., Imamura, F., Tsuji, Y., Matsutomi, H., Tinti, S., Cook, B., Chandra, Y. P. and Usman, M. 1995. Damage conditions of East Java Tsunami of 1994 analyzed. *EOS Trans. Am. Geophys. Union*, 76 (26), 257–264.

Yeh, H., Imamura, F., Synolakis, C., Tsuji, Y., Liu, P. L.-F. and Shaozhong, S. 1993. The Flores Island Tsunami. *EOS Trans. Am. Geophys. Union*, 74 (33), 369, 371–373.

Yeh, H. 2014. Personal communication, April 1, 2014 06:20 CET.

Yuan, Z. and Huang, Z. 2009. Solitary wave forces on an array of closely spaced circular cylinders. *Proceedings of 5th Int. Conf. Asian and Pacific Coasts*, Vol. 1, Singapore, pp. 136–142.

Zdravkovich, M. M. 1977. Review-review of flow interference between two circular cylinders in various arrangements. *J. Fluids Eng.*, 99 (4), 618–633.